ChemistryOpen

Research Article
doi.org/10.1002/open.202200201

Chemistry Europe
European Chemical Societies Publishing

www.chemistryopen.org

A Carbon Paste Electrode Modified by Bentonite and L-Cysteine for Simultaneous Determination of Ascorbic and Uric Acids: Application in Biological Fluids

Mohamed Choukairi,*[a] Dounia Bouchta,[a] Loubna Bounab,[b] Elisa González-Romero,[c] Mohamed Achache,[a] Khalid Draoui,[a] Faiza Chaouket,[a] Ihssane Raissouni,[a] and Mouad Gharous[a]

A novel modification of a paste carbon electrode by Bentonite (Bent) and L-Cysteine (L-Cyst) was carried out for uric acid (UA) and ascorbic acid (AA) detection and quantification. Morphological and compositional characterization of the electrode surface were carried out using electrochemical impedance spectroscopy (EIS), scanning electron microscopy (SEM) and energy dispersive X-ray spectroscopic analysis (EDS). Cyclic voltammetry (CV) and square wave voltammetry (SWV) techniques were used to analyze UA and AA. The obtained sensor shows a good stability, sensibility, selectivity, and regeneration ability. Accordingly, the limit of detection (LOD) is found to be 0.031 μM and 9.6 μM for UA and AA, respectively. A good linearity in the range of 0.1 to 100 μM for UA and 10 to 1000 μM for AA was obtained. The peak-to-peak separation of UA-AA ($\Delta E_{UA\text{-}AA}$) was determined to be 330 mV. In addition, the sensor is applied successfully to monitor UA and AA in serum samples.

Introduction

Uric acid (UA) and ascorbic acid (AA) are electroactive biomolecules of high medical interest, and plays a central role in the metabolism of human body.[1] AA, commonly known as vitamin C, is a water-soluble vitamin present in high amounts in the body and in various products including those of animal and vegetable origin.[2] In apparently healthy subjects, the physiological concentration of AA in blood serum is in the range of 34–113 μM.[3] AA plays several roles in the human body thanks to its antioxidant and hydroxylating properties.[2] It is an antioxidant molecule used for the repair and growth of bodily tissues and commonly used as supplement to maintain an adequate intake of vitamins.[2,4] It intervenes in the synthesis of collagen, tyrosine, carnitine, cholesterol, and bile acids.[2] AA reacts directly with the species reactive oxygen and nitrogen and reduces the superoxide anion under acidic or basic conditions.[2] It is also involved in iron metabolism and plays a role in removing carcinogens and carcinogenic nitrosamines.[2,5] AA can also inhibit lipid peroxidation reacting with peroxyl radicals and oxo-ferry complex.[6] It is also involved in several enzymatic reactions and in the organism's defense mechanisms against several pathologies.[7]

UA is produced by the decomposition of purines in the organism.[8] An excessive synthesis of UA or urinary excretion defect can lead to an excessive accumulation of UA in the blood, which is related to the apparition of various diseases like gout, hyperuricemia, diabetes and hypertension.[9] UA has been suggested to provide a high radical scavenging activity.[10] The concentration of UA in a healthy human is in the range of 140–400 μM in blood, 240–520 μM in serum, and 1500–4500 μM in urine.[11] In the lacrimal fluid, UA is considered as the first barrier protecting the cornea against oxidative damage by photodynamic reactions and toxic chemicals.[12] UA is found in higher concentrations than AA in the body, bringing about two thirds of the antioxidant capacity of plasma.[13] In the presence of AA, they can both contribute to more than 80% of antioxidant activity of the plasma.[13] Both UA and AA are often co-present in human biological fluids, especially blood and urine.[14]

Various analytical approaches are employed to monitor UA and AA, such as electrochemiluminescence, fluorescence methods, high performance liquid chromatography capillary electrophoresis, isotope dilution mass spectrometry, and others.[15] However, most of these techniques have several limitations namely for the analysis of complex biological fluids.[16] These shortcomings include complexity, high cost, low sensitivity, and non-selectivity.[15b] Therefore, to overcome all these limitations, electrochemical techniques can provide a very attractive

[a] Prof. Dr. M. Choukairi, Prof. Dr. D. Bouchta, Prof. Dr. M. Achache, Prof. Dr. K. Draoui, Prof. Dr. F. Chaouket, Prof. Dr. I. Raissouni, Dr. M. Gharous
Laboratory of Materials and Interfacial Systems
Faculty of Science
Abdelmalek Essaadi University
B.P. 2121, 93002 Tetouan (Morocco)
E-mail: mchoukairi@uae.ac.ma
[b] Prof. Dr. L. Bounab
Laboratory of Information System and Software Engineering
National School of Applied Sciences of Tetouan
Abdelmalek Essaadi University
93000 Tetouan (Morocco)
[c] Prof. Dr. E. González-Romero
Department of Analytical Chemistry and Food
University of Vigo-Campus
36310 Vigo (Spain)

alternative.[15b,16] However, the simultaneous detection of AA and UA by several conventional electrodes poses a problem of overlapping oxidation signals as both acids have very close oxidation potentials.[17] Modified carbon paste electrode (CPE) are a category of electrodes that have several advantages such as simplicity, selectivity, high stability, and good biocompatibility.[18] Owing to these advantages, modified CPEs have widely been used for the determination of several chemical and biochemical molecules such as UA, AA, dopamine (DA), glucose, heavy metal ions, and so on.[15b,19]

Bentonite (Bent) is a clay composed principally of montmorillonite.[20] This material has very attractive properties for electrochemical analysis such as a high cation exchange capacity, high specific surface area, chemical and physical stability, and tendency to react with various organic and inorganic compounds.[21] L-Cyst ($HSCH_2CH(NH_2)COOH$) is a peptide molecule that can be used for improving the electron transfer reaction in free-mediated biosensors.[22] In addition, the modification of electrode by L-Cyst leads to development of analytical performance such as the overpotential and the increase of the sensitivity towards UA, AA, epinephrine, and chlorpromazine.[23]

In this context, we have taken advantages of the simultaneous properties of carbon, Bent, and L-Cyst to develop a carbon paste electrode (CPE) modified with Bent and L-Cyst to efficiently apply in the analysis of AA and UA. In this work, we have adopted an easy, inexpensive, very simple, and few-step method to design a very reliable and efficient electrochemical sensor system. The separation of the oxidation peak potentials for AA and UA are large enough to determine these molecules individually and simultaneously with remarkable sensitivity. The L-Cyst/Bent/CPE electrode provides very acceptable values of repeatability, reproducibility, and excellent stability. Further, this sensor can be efficiently applied in the simultaneous detection of AA and UA in complex mixtures such as chemical and biological samples.

Experimental Section

Reagents

AA was obtained from Aldrich (Milwaukee, USA), UA was obtained from Sigma (Spain), L-Cyst was obtained from Fluka Chemical Company (Switzerland), H_2SO_4, and HCl were bought from Panreac (Spain). NaOH, KH_2PO_4, and K_2HPO_4 were purchased from Fluka (Spain) for preparation of phosphate buffer solution (PBS). Paraffin oil was obtained from Fluka, Plastic (PVC) capillary tubes (i.d. 2 mm) were used as composite's bodies. Serum with serum group (A) rhesus negative was provided by blood transfusion center, Tetouan, Morocco. Graphite powder (spectroscopic grade RBW) was obtained from SGL Carbon (Ringsdorff, Germany). Bentonite was bought from Segangane, Nador, Morocco. All experiments were carried out at room temperature and all reagents were of higher analytical degree.

Apparatus

A potentiostat/galvanostat type Voltalab PGZ301 (DYNAMIC – EIS VOLTAMMETRY – France) controlled by a computer was used for voltammetric measurements. The chemical data was transformed into electrical signals by means of voltamaster software. The three-electrode single-compartment cell contained a reference electrode Ag/AgCl (in saturated KCl solution), a platinum wire as the counter electrode and the modified electrode (L-Cyst/Bent/CPE) as a working electrode. Cyclic voltammetry (CV), square wave voltammetry (SWV), and electrochemical impedance spectroscopy (EIS) were used as analytical techniques. Scanning electron microscopy (SEM) and energy dispersive X-ray spectroscopy (EDS) analysis was performed in an SH 4000 M (BRUKER Company, HIROX, Oregon, JAPON) and used to characterize the electrodes before and after modification.

Preparation of bare and modified carbon paste electrodes

L-Cyst/Bent/CPE was prepared by thoroughly hand mixing 4 g of graphite powder, 0.4 g of Bent, and 0.3 g of L-Cyst with an appropriate amount of mineral oil in an agate mortar by using a pestle to have a homogeneous mixture. The latter was inserted in a plastic cylindrical tube with a thickness of one centimeter. To establish electrical contact with the external circuit, a copper wire was inserted and fixed in the paste. Unmodified and modified CPE by Bent (Bent/CPE) were prepared in a similar way with the exception of omitting Bent and L-Cyst for the (CPE) and L-Cyst for (Bent/CPE). The electrode surface was rinsed with ethanol and distilled water. Finally, the electrodes surface was cleaned electrochemically by the application of a number of cyclic voltammograms.

Results and Discussion

Effect of Bent and L-Cyst percentages on the response of the L-Cyst/Bent/CPE

One of the first parameters to take into account when preparing a modified CPE is the percentages of Bent and L-Cyst in the final composition of the mixture. Different percentages of Bent (2.5%, 5%, 7.5%, 10%, 15%, and 20% (w/w)) were added to the paste carbon composition so as to investigate their effect on the electrode response (Figure 1A). Furthermore, different amounts (5%, 7%, 10% (w/w)) of L-Cyst were added to the mixture at the optimal Bent/carbon mixture composition (10% (w/w)) (Figure 1B). The SWV responses of the modified and unmodified electrode were compared.

Figure 1A shows that the response is remarkably influenced by the Bent content. The signal increases with increasing Bent percentage until reaching its maximum value at 10%. The electrochemical response obtained at 10% Bent/CPE is three times better than CPE. This improved response is related to the high number of active sites and the high electron transfer across the 10%Bent/CPE/electrolyte interface. Therefore, the conductivity of the electrode decreases at higher Bent percentages which is ascribed to the lower carbon content. Figure 1B, illustrates the effect of the L-Cyst content ranging from 0% to 10% upon 100 μM UA. The peak current obtained at 7%L-Cyst/10%Bent/CPE was found to be 27 and 85 times higher than the

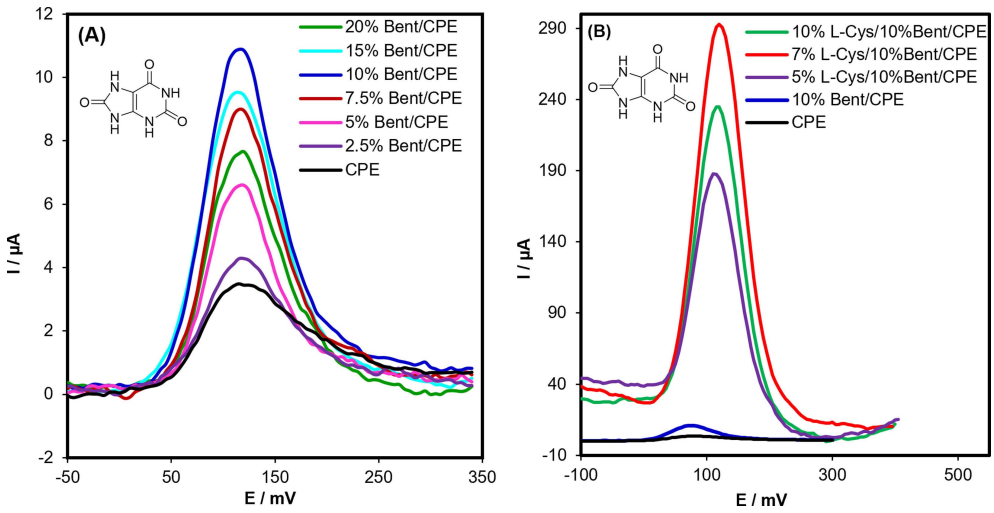

Figure 1. SW voltammograms of 100 µM UA in a solution of phosphate buffer (pH 7) at electrodes: (A) Bent/CPE at percentages of clay. (B) 10% Bent/CPE modified by different percentages of L-Cyst.

ones obtained at 10%Bent/CPE and at CPE, respectively. However, a significant lowering of the voltammetric response was noted when the concentration of L-Cyst was greater than 7% due to the saturation of active sites occupied by the molecules of L-Cyst and the creation of a barrier to electron transfer. These results show that the presence of Bent (10%) and L-Cyst (7%) in the mixture lead to a remarkable improvement in the voltammetric response. Consequently, the 7%L-Cyst/10%Bent/CPE (L-Cyst/Bent/CPE) was selected as optimum for further experimentations.

EDS and SEM analysis of CPE, Bent/CPE and L-Cyst/Bent/CPE

SEM and EDS techniques were used to confirm the modification of carbon paste, and to explore the eventual differences between the morphological features of the bare carbon paste surface and the modified electrode by Bent and L-Cyst/Bent. Figure 2 shows SEM micrographs and EDS spectra for the unmodified (CPE) (A and D) and modified electrodes with Bent (Bent/CPE) (B and E) and with Bent and L-Cyst (L-Cyst/Bent/CPE) (C and F). The SEM images showcase the morphological differences of the three electrode surfaces (Figure 2 A, B, C). This modification is also proved by the appearance of five new

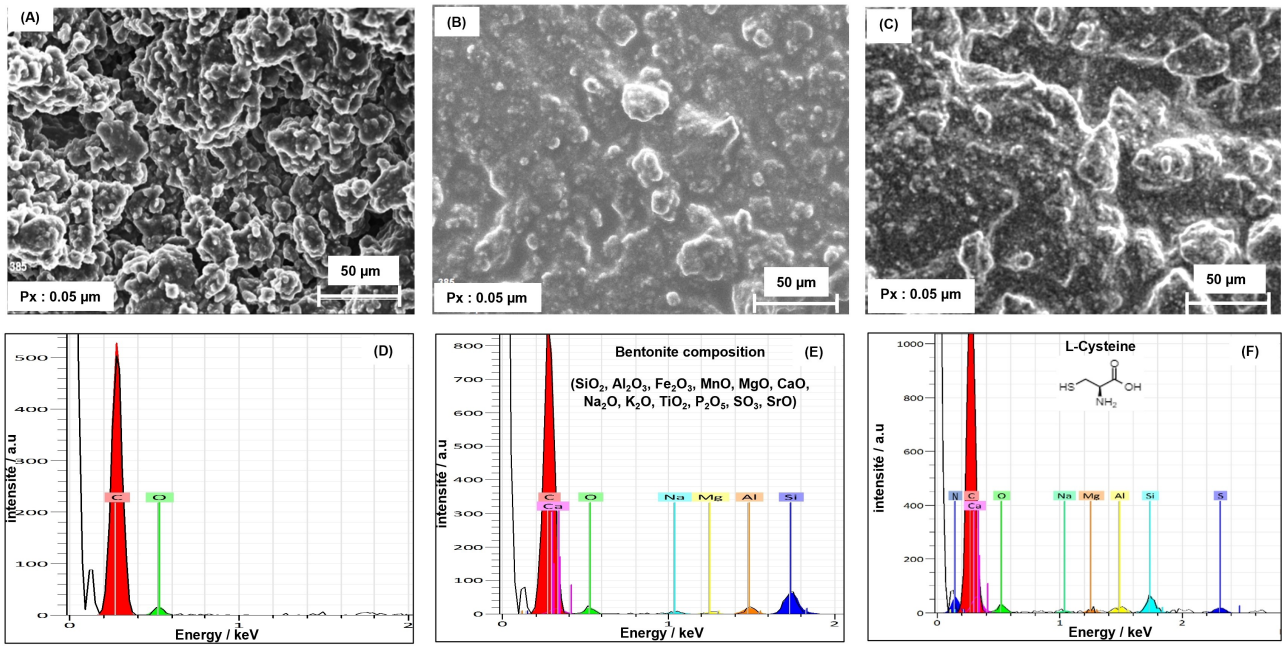

Figure 2. SEM micrograph and EDS spectrum of (A and D) CPE (B and E) Bent/CPE (C and F) L-Cyst/Bent/CPE.

peaks corresponding to Si, Mg, Na, Al, and Ca belonging to the Bent composition in the EDS spectrum (Figure 2E). The modification of the electrode by L-Cyst was also proved by the existence of sulfur and nitrogen in the mixture of the modified electrode (Figure 2F). All these results reveal that the modification of the electrodes was successful.

Electrochemical impedance study

EIS (Electrochemical impedance spectroscopy) is used to aid the electrochemical characterization of the sensor surface. Figure 3 shows the Nyquist plots of EIS for (a) bare CPE, (b) Bent/CPE and (c) L-Cyst/Bent/ CPE in a solution of 5 mM $[Fe(CN)_6]^{3-/4-}$. The three impedance spectra obtained corresponding to the three electrodes are characterized by two parts: the first part is a semi-circle in the high frequency region, associated with a charge transfer at the electrode surface/solution interface and characterized by a charge transfer resistance. The second is the straight line recorded at low frequency which indicates a diffusion-controlled process at the electrode surface.

The electron transfer resistance (R_{ct}) is estimated to be 1300 $\Omega\,cm^{-2}$ for the bare CPE. This value dropped to 700 $\Omega\,cm^{-2}$ for Bent/CPE and to 578 $\Omega\,cm^{-2}$ for L-Cyst/Bent/CPE. These results show that the value of the charge transfer resistance R_{ct} is lowered for each modification step, which demonstrates that the presence of Bent and L-Cyst facilitate charge transfer at the interface. It can also indicate the successful modification of the L-Cyst/Bent/CPE mixture.

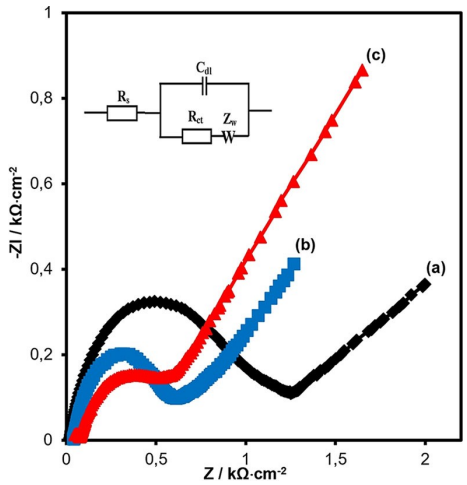

Figure 3. Nyquist plots of 5 mM $[Fe(CN)6]^{3-/4-}$ at bare CPE (a), Bent/CPE (b) and L-Cyst/Bent/CPE (c). Frequency range: 100 kHz–5 mHz. AC potential ±5 mV. Inset: The Rundles equivalence circuit model used to fit the experimental data.

Variables Optimization

pH effect on UA and AA oxidation

The influence of solution pH on current peak and potential during UA and AA (50 μM) oxidation was studied using 50 mM PBS at different pH values (Figure 4). The potential peaks for UA and AA were shifted to a lower value with increasing pH values, that is, the peak potentials were moved from 390 mV to −10 mV for UA (Figure 4A and a) and from 230 mV to <M-< 115 mV for AA (Figure 4B and b), indicating that protons were directly involved in the overall oxidation reactions. The linear regression equations for UA and AA are $E_{UA}/mV) = -59.553$ pH $+518.85$ ($R = 0.993$) and $E_{AA}/mV) = -53.571$ pH $+310.71$ ($R = 0.998$), respectively (Figure 4a, 4b). The calculated slopes of 59 mV/pH for UA and 54 mV/pH for AA are equal (for UA) and close (for AA) to the theoretical value of 59 mV/pH. According to the Nernst equation, these results reveal that the number of electrons and protons is equal to each other in the oxidation mechanism of UA an AA.[24]

Figure 4 also shows that the variation in pH values has a remarkable effect on the current peak intensity. concerning UA the maximum value of the intensity is attained at pH 2, then lessened slightly as the pH increases from 2 to 5 and has risen again at pH from 5 to 7. It then decreases slowly with rise in pH from 7 to 8.5 (Figure 4a). The maximum current peak intensity of AA appears at pH 4 and decreases slightly at pH values higher than 4 (Figure 4b). The peak current intensity variation at different pH values can be explained by the presence of electrostatic interactions between the analytes present in the solution and the ionic surface groups.[25] These interactions depend on the equilibrium between the ionic and molecular form of the electrolytes and surface compounds, this equilibrium depends on the pH values of the solution and the pK_a values of the chemical species. Considering the physiological pH (pH 7.4) and results obtained, pH 7 PBS was chosen for the following experiments.

The scan rate effect on current intensity and potential peaks

The influence of the scan rate on the peak current intensity was investigated using CV in order to study the kinetics of electrode reaction. The Figure 4 shows CV curves obtained on L-Cyst/Bent/CPE in PBS 50 mM (pH 7) with UA (500 μM) (Figure 5A) and AA (1000 μM) (Figure 5B) in a scan rate range from 25 to 300 $mV\,s^{-1}$. The peak current intensity was proportional to the scan rate for UA (Figure 5a), and to the square root of the scan rate for AA (Figure 5b). These findings show that the oxidation reactions of AA on the electrode surface are controlled by diffusion phenomenon while the oxidation reactions of UA are controlled by adsorption.

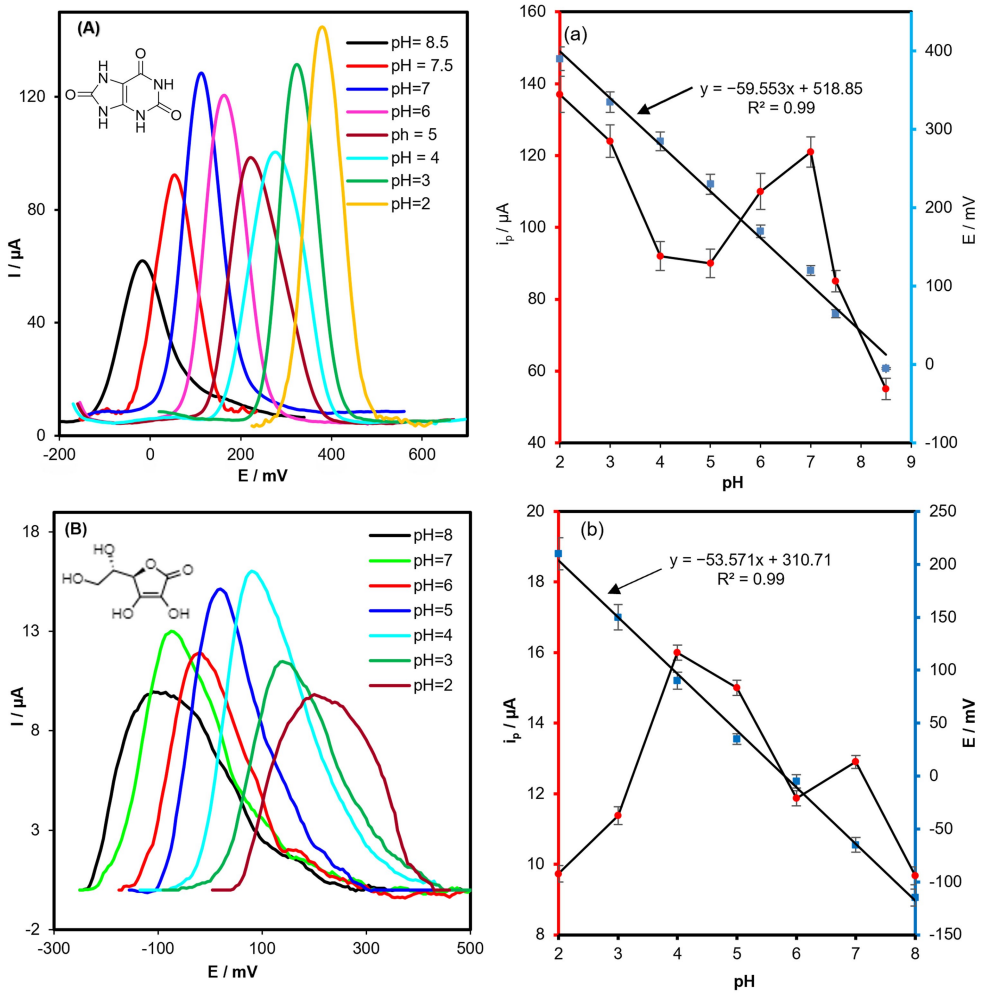

Figure 4. SW voltammograms obtained at the L-Cyst/Bent/CPE in the range of pH 2→8.5 (UA) and 2→8 (AA) in 50 mM PBS including 50 µM of UA (A) and AA (B) at a scan rate of 50 mV s^{-1}. inset: Effect of pH on Ep (■) and i_p (●).

The impact of accumulation time on SWV peaks of UA and AA

The accumulation time has been studied to obtain a much more sensitive peak current. The electrochemical sensor was dipped in a PBS solution (pH 7) containing UA (500 µM) or AA (50 µM). The results obtained in Figure 6 illustrate how the current peak intensity varies with the accumulation time at open-circuit potential with stirring. This result demonstrates that the process of incorporation of UA (a) is rapid. During the first minutes, the intensity of the oxidation peak current increased rapidly and stabilized after 5 to 6 min of incubation. This time was maintained during the rest of the assays for UA to ensure the reproducibility of the results. Concerning the AA (b), the process of incorporation is found to be very rapid since the peak current intensity remains invariable with the accumulation time variation.

Electrochemical oxidations of UA and AA at L-Cyst/Bent/CPE

To determine the electrode sensitivity, limit of detection (LOD) and linear range, the effect of the concentration of UA (Figure 7A) and AA (Figure 7B) on peak current intensity was investigated. It is found that the peak current intensity varies linearly with the variation of the two acids' respective concentrations (Figures 7a and 7b). The linearity range of the concentration is 0.1 to 100 µM for UA and 10 to 1000 µM for AA. This linearity follows the equation: $i_p/\mu A = 10.419 + 1.8026\, C_{UA}/\mu M$ ($R^2 = 0.9904$) for UA and $i_p/\mu A = 4.8281 + 0.0724\, C_{AA}/\mu M$ ($R^2 = 0.9943$) for AA. The LOD value is found to be 0.031 µM for UA and 9.6 µM for AA, and limit of quantification (LOQ) value is found to be 0.1 µM for UA and 32 µM for AA. The formula used to calculate the LOD and LOQ values is LOD = 3*(SD/a) and LOQ = 10*(SD/a) in which SD is the standard deviation (SD = 0.12 for UA and SD = 0.34 for AA), and a is the slope of the calibration curve. Consequently, this lower LOD can be achieved using the proposed modified electrochemical sensor.

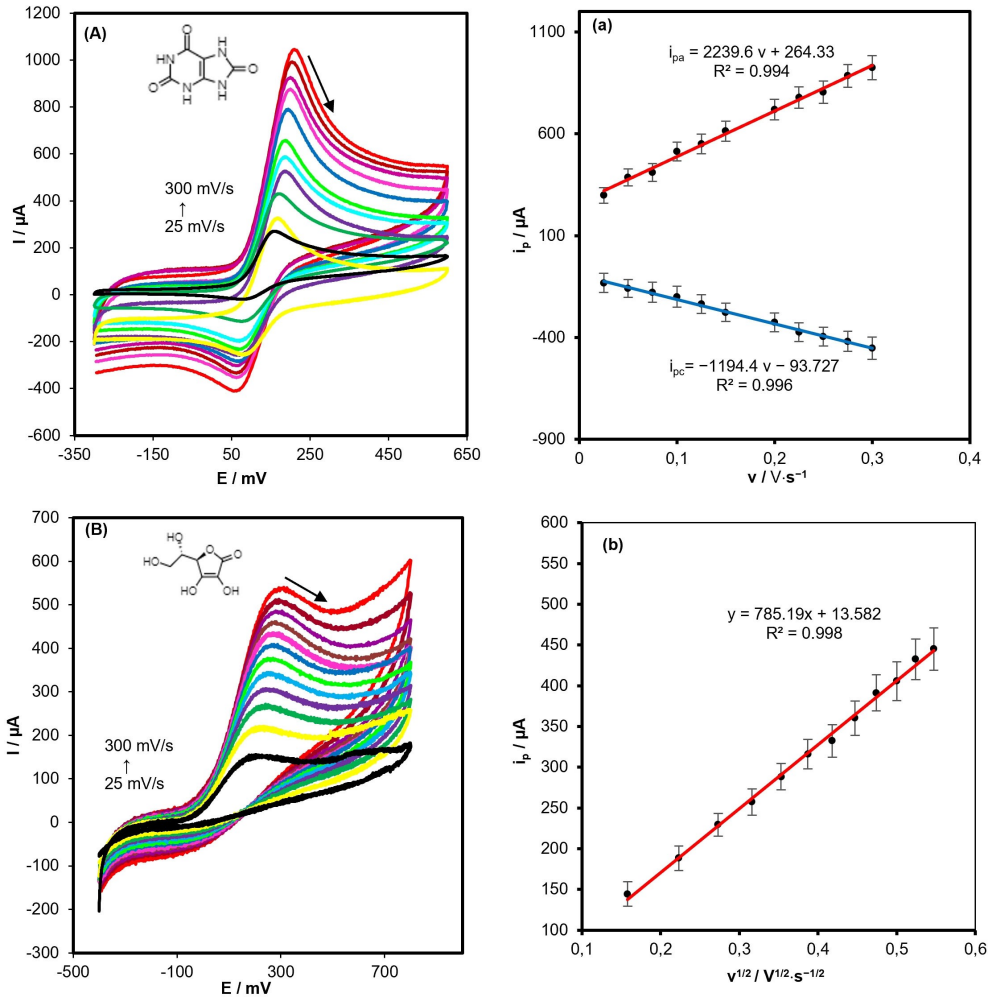

Figure 5. CV curves at different scan rate values: (A) 500 µM UA, ((a) anodic and cathodic peak current, i_{pa} and i_{pc}, vs. v) and (B) 1000 µM AA ((b) anodic peak current, i_{pa} vs. $v^{1/2}$) on L-Cyst/bent/CPE electrode at different scan rates in 50 mM PBS (pH 7).

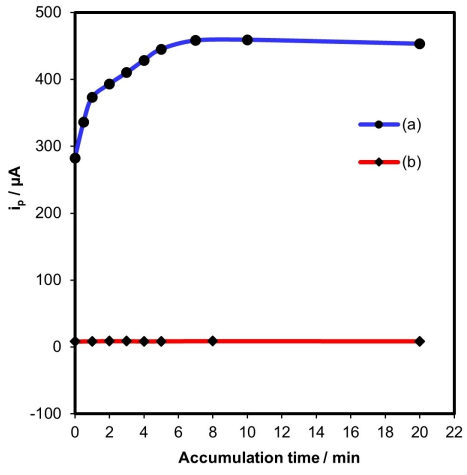

Figure 6. Optimization of open circuit accumulation time on the response of L-Cyst/Bent/CPE modified electrode for (a) UA (500 µM) and (b) AA (50 µM) using SWV technique in 50 mM PBS (pH 7) and 50 mV s^{-1} scan rate.

These limits allow detecting physiological changes of both targets, since literature has reported that physiological serum concentration for a healthy human is between 34 and 113 µM for AA[3] and between 240 and 520 µM for UA.[11] L-Cyst/Bent/CPE seems to have a good performance concerning its linear range, LOD, and electrocatalytic activity at the modified electrode surface for the UA and AA oxidation. Therefore, the proposed sensor is appropriate for UA and AA determination in clinical research.

Repeatability, reproducibility, stability, and selectivity of the sensor

To investigate the repeatability of the L-Cyst/Bent/CPE sensor, the measurements of the SWV response were further performed for six selected electrodes toward UA (1 µM) and AA (100 µM). The calculated relative standard deviations (RSD) were 4.1% and 4.8% for UA and AA, respectively. These results indicate a good repeatability of the sensor response. The reproducibility was also tested through a series of five electrodes prepared under the same conditions and then applied for the detection of UA and AA. The RSD to the peak current intensity of the SWV

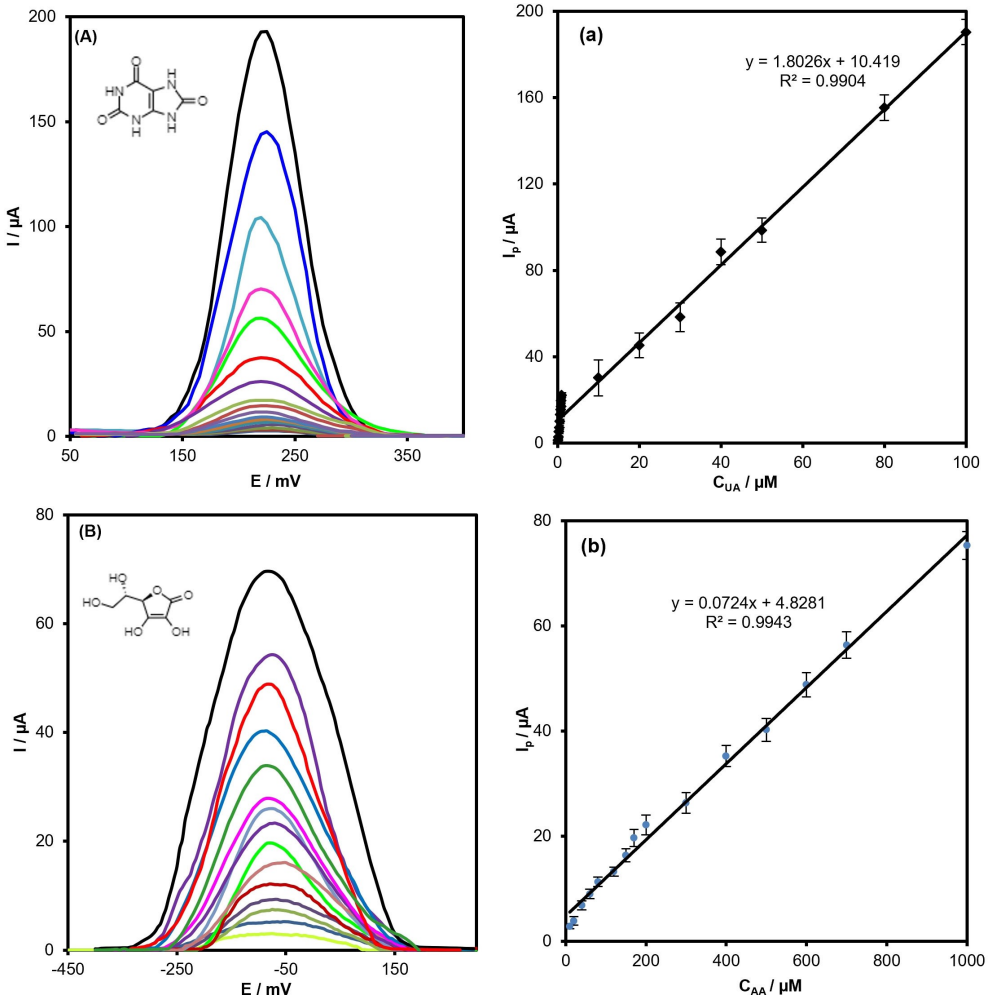

Figure 7. SW voltammograms obtained for different concentrations of (A) UA (0.1 to 100 µM) and (B) AA (10 to 1000 µM) on L-Cyst/Bent/CPE in 50 mM PBS (pH 7). (a and b) linear variation of the peak current intensity with the UA and AA concentrations, respectively.

measurements for the five electrodes were 5% for UA and 6.2% for AA. These results indicate that the L-Cyst/Bent/CPE is highly reproducible for UA and AA sensing. The storage stability of L-Cyst/Bent/CPE was also examined by the SWV response for 1 µM UA and 100 µM AA in 50 mM PBS (pH 7). The sensor was rinsed with PBS then stored at room temperature (20 °C to 25 °C) after every dosage. A lowered voltametric response of the L-Cyst/Bent/CPE of 5% to 8% was noted after three weeks for UA and AA, respectively. According to these results, the modified electrode showed a remarkable repeatability, reproducibility and stability. The selectivity of the modified electrode is more critical for its usefulness in practical applications. Thus, in order to be used further in real samples, the sensor has been tested in the presence of the main common co-existing substance (DA) which could interfere with the detection of AA and UA in biological fluids. The electrochemical responses of modified and unmodified electrodes toward ternary mixture of UA, DA and AA, the SWV measurements of bare CPE and L-Cyst/Bent/CPE were performed at the presence of 25 µM of UA, 50 µM of DA and 500 µM of AA in a PBS 50 mM (pH 7) (Figure 8). Practically no peak was observed for the unmodified

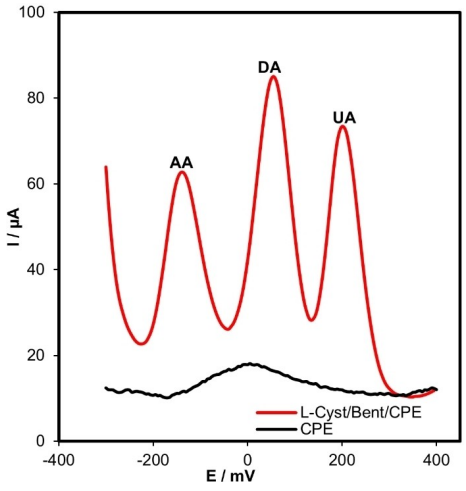

Figure 8. SW voltammograms obtained for 25 µM of UA, 50 µM of DA and 500 µM of AA at L-Cyst/Bent/CPE in a PBS 50 mM (pH 7).

CPE. However, on L-Cyst/Bent/CPE, three strong and well-separated oxidation peaks were observed at −135, 60 and

205 mV, respectively, corresponding to the electrooxidation of AA, DA and UA. The results show that the L-Cyst/Bent/CPE allows the identification of AA, UA, and DA with good selectivity.

Interference study

Determination of UA and AA simultaneously at the L-Cyst/Bent/CPE

UA and AA coexist in both the blood serum and extracellular fluid of the central nervous system,[26] and the oxidation potential values of these two species are very close to each other. Therefore, the selective detection of these acids is a challenging task.

To complete the performance validation of our sensors, it seems interesting to explore its behavior against a binary mixture AA-UA solution. Figures 9A and B illustrate the evolution of the voltammograms of 50 μM UA at the L-Cyst/Bent/CPE in the presence of 1000 μM of AA. At the bare electrode (CPE), no evident corresponding re-oxidation peak is observed. In contrast, at the modified electrode (L-Cyst/Bent/CPE), two sharp peaks at −165 mV and 215 mV were observed, corresponding to AA and UA oxidation, respectively. A clear separation is observed between the two current peaks with voltage peak separation of 375 mV. From an analytical point of view, this result is sufficient to confirm that the modified electrode allows a simultaneous detection of the target analytes.

SWV was used to measure the different concentrations of the two substances at the L-Cyst/Bent/CPE to examine the interference of UA and AA. In this analysis, the concentration of one of the two substances was modified, whereas the concentration of the other remained unchanged.

Figure 9A depicts the variation of the peak current intensity with the concentration of UA in the range of 0.1 μM to 100 μM. The concentration of AA was fixed at 500 μM. A linear relationship between the peak current and the concentrations of UA is observed (Figure 10a). The LOD is calculated as 0.031 μM (S/N = 3) for UA. Figure 10B shows the SWV response of AA oxidation in the concentration range from 10 μM to 1000 μM in the presence of 50 μM UA. As we can observe from the curves, the redox peak current intensity of UA varies linearly with the concentration (Figure 10b). The LOD was calculated as 9.6 μM (S/N = 3) for AA. The peak current intensity of the UA oxidation remained constant. In addition, the values of LOD and the linear range are competitive in comparison with those published in several works (Table 1).

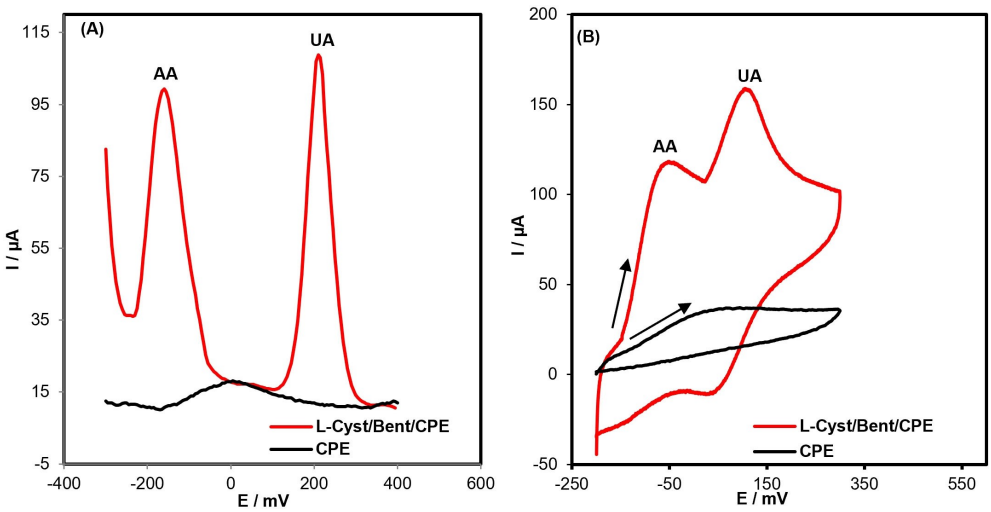

Figure 9. A) SW voltammograms and B) CV curves ($v = 0.1\ V\,s^{-1}$) obtained for 50 μM of UA and 1000 μM of AA at L-Cyst/Bent/CPE in a PBS 50 mM (pH 7).

Table 1. L-Cyst/ Bent/CPE performances in detection of UA and AA compared to other modified electrodes.

Modified electrode	Peak potential E [mV]		Linear range [μM]		Detection limit [μM]		Ref.
	UA	AA	UA	AA	UA	AA	
sonogel–carbon	10	140	10–100	50–1000	10	50	[23a]
Mn-SnO_2/GCE	250	110	0.5–900	1–860	0.36	0.058	[27]
μAu-PEDOT	308	−94	2–600	5–300	1.5	2.5	[28]
H-GO/GCE	380	50	0.5–50	1–100	0.17	0.3	[29]
HNCMS/GCE	290	−50	5–30	100–1000	0.04	0.91	[30]
Pd-CNFs/CPE	–	–	2–200	50–4000	0.7	15	[31]
ZnO/CPE	420	190	0.7–1000	0.9–100	0.028	0.013	[32]
ACBK/GCE	380	110	1–20	50–1000	0.5	10	[33]
L-Cyst/Bent/CPE	215	−165	0.1–100	10–1000	0.031	9.6	This work

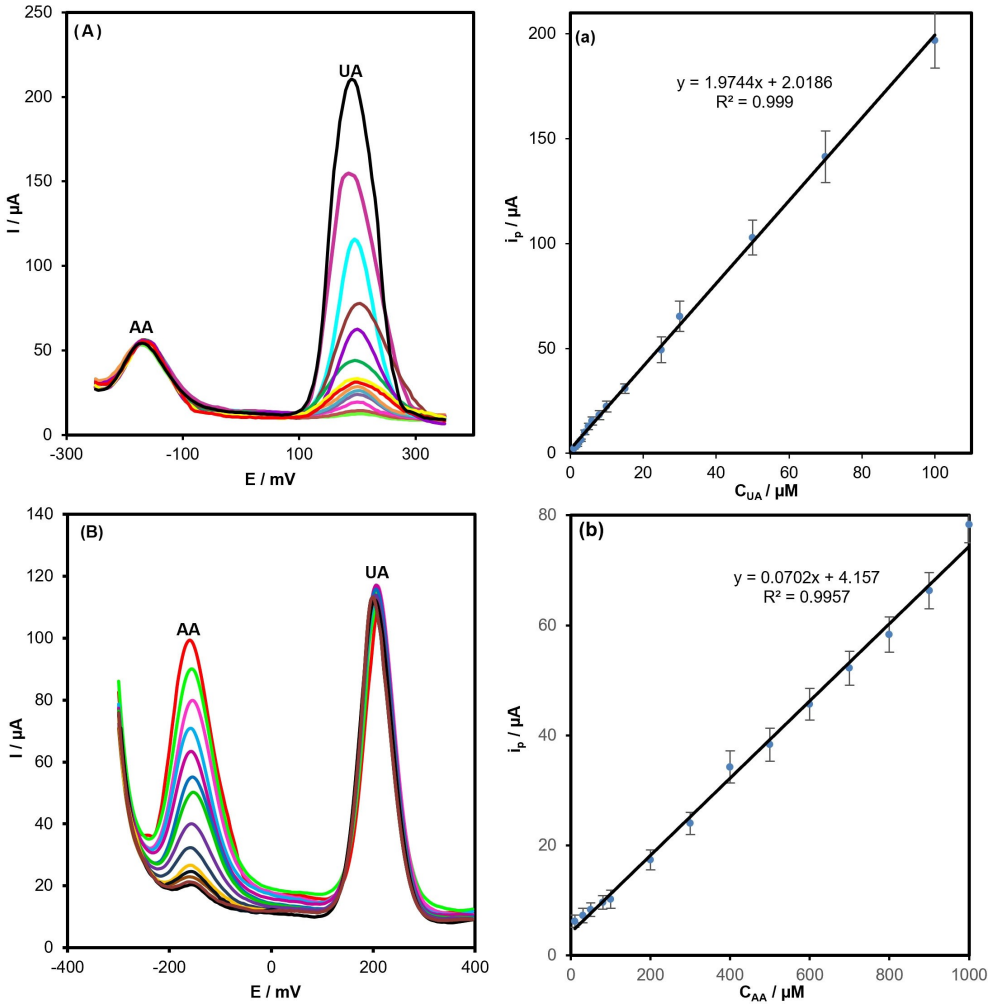

Figure 10. SW voltammograms obtained at L-Cyst/Bent/CPE in a PBS 50 mM (pH 7) (A) for 500 µM of AA and 0.1 to 100 µM of UA, (B) for 50 µM of UA and 10 to 1000 µM of AA, (a and b) linear variation of the peak current intensity with the UA and AA concentrations, respectively.

Compared to the results in terms of sensor sensitivity obtained during individual dosing for these two targets, we observe that the AA signal remains almost unchanged while it increases for UA. This increase in peak current intensity values is due to an "EC" mechanism resulting from a chemical reaction in solution coupled to the electrochemical step.[34] To clearly show this proposition, we dosed the AA-UA mixture again, we fixed the concentration of AA, we varied the concentration of the UA, and we kept the same solution all along the dosages to follow the intensities of the peaks. Figure 11A illustrates the curves of the peak current intensity of the two molecules as a function of UA concentration. Regarding AA, the peak current intensity varies inversely with the concentration of UA. The decrease in peak current intensity of AA presented in Figure 10 again confirms the existence of an electrochemical-chemical mechanism (EC) leading to UA regeneration. This mechanism consists of an electron transfer step allowing the production of the oxidized form of UA at the electrode surface, hence AA reduces the oxidized UA in a coupled chemical reaction ©, the reduced UA is regenerated near the electrode area. This explains the decrease in concentration of AA, which is not caused by interference phenomenon. This finding proves a very good selectivity of this electrode towards AA and UA.

Other experiments have been carried out to demonstrate this mechanism, since we evaluated the sensitivity of the proposed sensor to UA detection in the presence and the absence of an excess of AA. The calibration curves in the two cases were compared. Figure 12 shows the plot of calibration curves of the increasing concentrations of UA in the presence and absence of AA in the pH 7 PBS. In the presence of AA, the current intensity of the UA oxidation peak increases substantially. Therefore, the peak current intensity relative to UA oxidation in the presence of AA (b) is superior to its oxidation in absence of AA (a). This result confirms that the increase in the peak intensity of UA oxidation in presence of AA resulted from a chemical regeneration of UA and is not caused by an interference process between the two substances response, which confirms the existence of the EC mechanism.

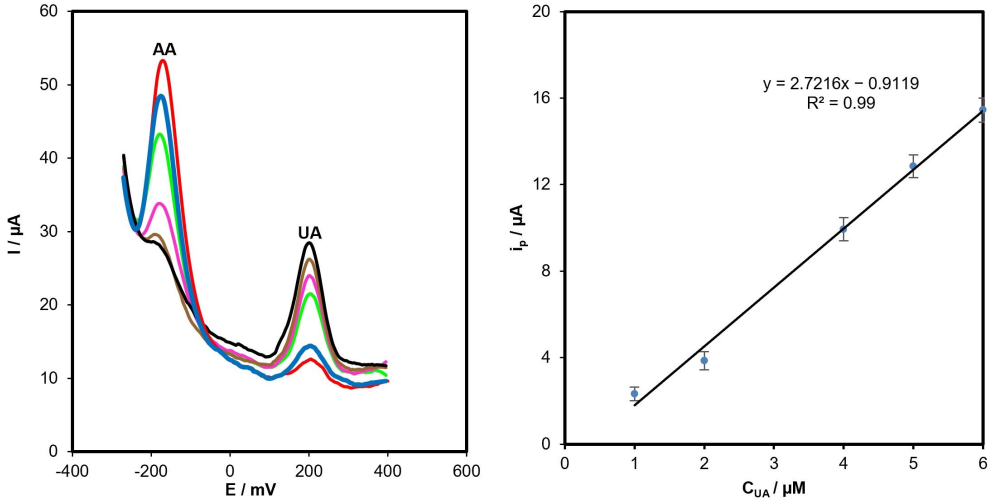

Figure 11. (A) SW voltammograms obtained at L-Cyst/Bent/CPE in a PBS 50 mM (pH 7) for 500 µM of AA and 1 to 6 µM of UA, (a) linear variation of the peak current intensity with the UA concentrations.

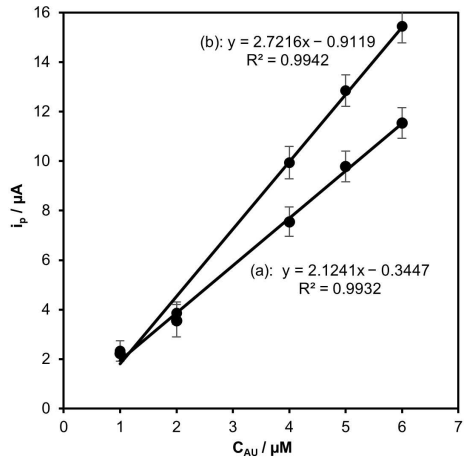

Figure 12. Linear fits of calibration of UA on L-Cyst/Bent/CPE in SWV in absence (a) and in presence (b) of AA at 500 µM.

Real sample analysis

The sensor was tested for conducting UA and AA analysis in serum samples to confirm the use of the L-Cyst/Bent/CPE sensor in real samples. The results of this analysis are reported in Table 2. The recovery values of the enriched samples for AA and UA are in the range of 97.14–102% and 97.34–104%, respectively. Clearly, the prepared sensor can successfully be used for the detection of AA and UA in biological samples.

Table 2. Results of the determination of UA and AA in a sample of human serum at L-Cyst/Bent/CPE.

Human serum	Added [µM]		Found [µM]		Recovery [%]	
	UA	AA	UA	AA	UA	AA
	–	–	–	nd[a]	–	–
	0.05	20	0.0512	20.8	102.4	104
	0.07	50	0.068	48.67	97.14	97.34
	0.1	80	0.102	78.65	102	99.31

[a] nd: not detected.

Conclusions

In this present study, a new CPE modified by Bent and L-Cyst was elaborated for UA and AA analysis. The obtained sensor was developed using a very fast, simple, and inexpensive method. This system showed a high electrocatalytic effect, very high sensitivity, and excellent selectivity for individual and simultaneous detection of AA and UA. This sensor also provides a good affinity, fast response, very low value of the LOD, wide linear range, good storage stability, and very remarkable reproducibility. The L-Cyst/Bent/CPE can be effectively used for the detection of UA and AA in real samples (human blood serum). Furthermore, the proposed sensor has all the characteristics required to be exploited commercially for the electrochemical detection of AA and UA and other substances in real samples such as lakes, wastewater, milk, blood, urine, and drinking water.

Conflict of Interest

The authors declare no conflict of interest.

Data Availability Statement

Research data are not shared.

Keywords: ascorbic acid · bentonite · carbon paste electrode · L-cysteine · uric acid

[1] M. Asif, A. Aziz, H. Wang, Z. Wang, W. Wang, M. Ajmal, F. Xiao, X. Chen, H. Liu, *Microchim. Acta.* **2019**, *186*, 61.
[2] B. Mittu, Z. R. Bhat, A. Chauhan, J. Kour, A. Behera, M. Kaur in *Nutraceuticals and Health Care* (Eds. *J. Kour, G. A. Nayik*),Academic Press, Elsevier, **2022**, pp. 289–302.
[3] M. Malik, V. Narwal, C. Pundir, *Process Biochem.* **2022**, *18*, 11–23.
[4] A.-M. Yu, H.-Y. Chen, *Anal. Chim. Acta.* **1997**, *344, 181–185*.
[5] S. S. Mirvish, *Cancer* **1986**, *58*, 1842–1850.
[6] M. A. Sahari, S. B. Ardestani in *Frontiers in Natural Product Chemistry, Vol. 9* (Ed. A. ur-Rahman), Bentham Science Publishers, Singapore, **2022**, pp. 125–184.
[7] A. Renaud, *J. de Pediatrie et de Pueric.* **2003**, *16*, 281–283.
[8] J. Maiuolo, F. Oppedisano, S. Gratteri, C. Muscoli, V. Mollace, *Int. J. Cardiol.* **2022**, *213*, 8–14.
[9] R. El Ridi, H. Tallima, *J. Adv. Res.* **2017**, *8*, 487–493.
[10] B. N. Ames, R. Cathcart, E. Schwiers, P. Hochstein, *Proc. Nat. Acad. Sci.* **1981**, *78, 6858–6862*.
[11] a) F. Mazzara, B. Patella, G. Aiello, A. O'Riordan, C. Torino, A. Vilasi, R. Inguanta, *Electrochim. Acta.* **2021**, *388*, 138652; b) R. Jirakunakorn, S. Khumngern, J. Choosang, P. Thavarungkul, P. Kanatharana, A. Numnuam, *Microchem. J.* **2020**, *154*, 104624.
[12] J. Horwath-Winter, S. Kirchengast, A. Meinitzer, C. Wachswender, C. Faschinger, O. Schmut, *Acta Ophthalmol.* **2009**, *87*, 188–192.
[13] T. P. Whitehead, G. H. G. Thorpe, S. R. J. Maxwell, *Anal. Chim. Acta.* **1992**, *266*, 265–277.
[14] T. Rattanaumpa, S. Maensiri, K. Ngamchuea, *RSC Adv.* **2022**, *13*, 18709–18721.
[15] a) P. Zhang, X. Wu, H. Xue, Y. Wang, X. Luo, L. Wang, *Anal. Chim. Acta.* **2022**. *1212*, 339911; b) A. Azzouz, K. Y. Goud, N. Raza, E. Ballesteros, S.-E. Lee, J. Hong, A. Deep, K.-H. Kim, TrAC, *TrAC Trends Anal. Chem.* **2019**, *110*, 15–34.
[16] a) C. Retna Raj, T. Ohsaka, *J. Electroanal. Chem.* **2003**, *540*, 69–77; b) Ľ. Švorc, K. Kalcher, *Sens. Actuators B* **2014**, *194*, 332–342.
[17] a) K. Kunpatee, S. Traipop, O. Chailapakul, S. Chuanuwatanakul, *Sens. Actuators B* **2020**, *314*, 128059; b) H. Karimi-Maleh, O. A. Arotiba, *J. Colloid Interface Sci.* **2020**, *560*, 208–212; c) N. Mohammed Modawe Alshik Edris, J. Abdullah, S. Kamaruzaman, M. I. Saiman, Y. Sulaiman, *Arabian J. Chem.* **2018**, *11*, 1301–1312; d) A. Hatefi-Mehrjardi, M. A. Karimi, M. Soleymanzadeh, A. Barani, *Measurement.* **2020**, *163*, 107893; e) Y. V. M. Reddy, B. Sravani, S. Agarwal, V. K. Gupta, G. Madhavi, *J. Electroanal. Chem.* **2018**, *820*, 168–175; f) Y. V. M. Reddy, J. H. Shin, J. Hwang, D.-H. Kweon, C.-H. Choi, K. Park, S.-K. Kim, G. Madhavi, H. Yi, J. P. Park, *Biosens. Bioelectron.* **2022**, *214*, 114511.
[18] a) J. B. Raoof, R. Ojani, H. Beitollahi, R. Hossienzadeh, *Electroanalysis.* **2006**, *18*, 1193–1201; b) H. Beitollahi, J. B. Raoof, R. Hosseinzadeh, *Electroanalysis.* **2011**, *23*, 1934–1940; c) M. Mazloum-Ardakani, H. Beitollahi, M. K. Amini, F. Mirkhalaf, M. Abdollahi-Alibeik, *Sens. Actuators B.* **2010**, *151*, 243–249.
[19] M. Choukairi, D. Bouchta, L. Bounab, R. Elkhamlichi, F. Chaouket, I. Raissouni, I. Rodriguez, *J. Electroanal. Chem.* **2015**, *758*, 117–124.
[20] R. M. Carland, F. F. Aplan, *Mining Metall Explor.* **1995**, *12*, 210–218.
[21] I. E. Odom, *Philos. Trans. R. Soc. London.* **1984**, *311*, 391–409.
[22] S. Wang, D. Du, *Sensors.* **2002**, *2*, 41–49.
[23] a) M. Choukairi, D. Bouchta, L. Bounab, M. Benatyah, R. Elkhamlichi, F. Chaouket, I. Raissouni, I. N. Rodriguez, *J. Electroanal. Chem.* **2015**, *758*, 117–124; b) H. T. Purushothama, Y. Arthoba Nayaka, P. Manjunatha, R. O. Yathisha, M. M. Vinay, K. V. Basavarajappa, *Chem. Data Collect.* **2019**, *23*, 100268.
[24] C. Wang, Q. Liu, X. Shao, G. Yang, H. Xue, X. Hu, *Talanta* **2007**, *71*, 178–185.
[25] P. R. Roy, T. Okajima, T. Ohsaka, *J. Electroanal. Chem.* **2004**, *561*, 75–82.
[26] T. Cao, Y. Zhou, J. Zhang, H. Wang, L. Dong, Y. Zhang, L. Liu, Z. Tong, *Solid State Sci.* **2022**, *134*, 107058.
[27] N. Lavanya, E. Fazio, F. Neri, A. Bonavita, S. G. Leonardi, G. Neri, C. Sekar, *J. Electroanal. Chem.* **2016**, *770*, 23–32.
[28] F. Sekli-Belaidi, P. Temple-Boyer, P. Gros, *J. Electroanal. Chem.* **2010**, *647*, 159–168.
[29] H. L. Zou, B. L. Li, H. Q. Luo, N. B. Li, *Sens. Actuators, B.* **2015**, *207*, 535–541.
[30] C. Xiao, X. Chu, Y. Yang, X. Li, X. Zhang, *J. Chen, Biosens. Bioelectron.* **2011**, *26*, 2934–2939.
[31] J. Huang, Y. Liu, H. Hou, T. You, *Biosens. Bioelectron.* **2008**, *24*, 632–637.
[32] M. Arvand, S. Tajyani, *RSC Adv.* **2015**, *5*, 7222–7231.
[33] R. Zhang, G.-D. Jin, D. Chen, X.-Y. Hu, *Sens. Actuators B* **2009**, *138*, 174–181.
[34] F. Sekli-Belaidi, P. Temple-Boyer, P. Gros, *J. Electroanal. Chem.* **2010**, *647*, 159–168.

Manuscript received: September 20, 2022
Revised manuscript received: December 13, 2022